Innovations and Industrial Technologies 2025

Characterization of Spectrometer Burn Marks in Steel Alloys

Adrian Dera[1)], Szymon Witczak[1)]

[1)] Polytechnic Faculty, President Stanislaw Wojciechowski University of Kalisz

University of Kalisz

Kalisz, 23–24.10.2025

ABSTRACT

The aim of this study was to characterize spark spectrometer burn marks on steel samples and to determine the influence of alloying elements, particularly carbon, on the size, depth, and surface morphology of the burned areas. Seven iron-based steel reference samples were used in the research (designations: RG 13/411, RH 12/21, RN 13/74, RG 14/531, RH 18/46, RN 14/51, RH 31/31). The spark burns were performed using a Metal Lab Plus spectrometer by G.N.R., while surface topography analysis was carried out with aNanoscan 855 microscope by Jenoptic. A total of 35 burn areas were analyzed. The obtained data were statistically processed using the Pearson correlation coefficient to identify strong relationships between chemical composition and topographic parameters.

The results showed that elements such as molybdenum, niobium, antimony, cobalt, and vanadium exhibit a positive correlation with burn peak volume, while nickel, chromium, and cerium show a negative correlation. The volume of craters increased with higher content of lead, carbon, calcium, and manganese, but decreased with the presence of zinc, chromium, and nickel. Maximum burn depth increased with arsenic, magnesium, manganese, molybdenum, and niobium, while higher chromium and nickel content reduced it. Furthermore, molybdenum, nickel, and manganese were found to significantly affect the peak height and geometry of the burn marks.

In summary, the analysis confirmed strong correlations between the chemical composition of steel alloys and the parameters of spark burns. These findings can be applied to further optimize spectrometric analysis methods and to better understand the surface behavior and properties of iron-based alloys.

OBJECTIVES

The objective of this study was to investigate and characterize the morphology and parameters of spark burns generated by an optical emission spectrometer on steel alloy samples. The research aimed to determine the relationship between the chemical composition of iron-based alloys—particularly the carbon and alloying element content—and the resulting burn area dimensions, depth, and surface features. By analyzing the correlation between specific elemental concentrations and topographical parameters of the burn marks, the study sought to identify which elements most significantly influence the burn characteristics during spectrometric excitation. The ultimate goal was to enhance the understanding of the physical effects occurring during spark emission analysis and to support the optimization of spectrometric calibration and material characterization procedures for various steel grades.

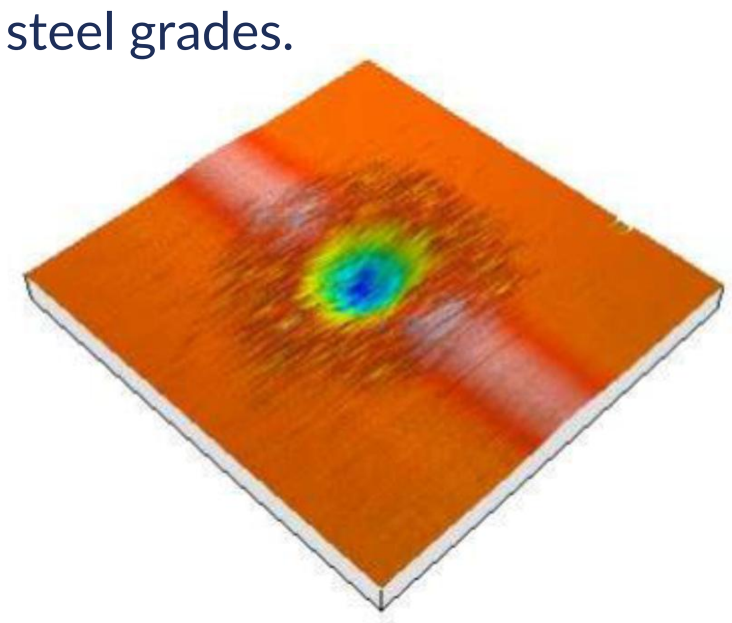

Example image of the surface topography of the burned area

CONCLUSIONS

Based on the conducted experiments and statistical analysis, several significant correlations were identified between the chemical composition of steel alloys and the parameters of spark burns generated during optical emission spectrometry. Elements such as molybdenum, niobium, antimony, cobalt, and vanadium exhibited a positive correlation with burn peak volume, while nickel, chromium, and cerium showed a negative correlation. The maximum burn depth increased with higher concentrations of arsenic, magnesium, manganese, molybdenum, and niobium, and decreased with greater amounts of chromium, nickel, copper, and zinc. Manganese appeared most frequently in strong or very strong correlations with grain area parameters, although clear dependencies were not always evident. Overall, the results confirmed that specific alloying elements significantly affect burn morphology and energy distribution, offering insights for refining spectrometric calibration and improving analytical precision in steel characterization.

Współczynnik Pearsona									
	Powierzchnia		Objętność		Max głębo/wysok		Średnia głębo/wysok		
Próbka	Otwór	Pik	Otwór	Pik	Otwór	Pik	Otwór	Pik	Pole Ziarno
C#1	-0,3839	0,7629	-0,2055	0,6542	0,3190	0,6065	0,1514	0,1879	-0,5041
Si#1	0,8389	-0,8234	0,6975	-0,7914	0,1037	-0,6369	0,2529	-0,5856	0,5177
Si#3	0,8401	-0,3562	0,6009	-0,3346	-0,0497	-0,1674	0,0256	-0,2674	-0,0460
Mn#10	0,1124	-0,3727	0,3295	-0,4070	0,5549	-0,6747	0,5655	-0,3464	0,4223
Mn#4	0,7197	0,0687	0,5577	0,0337	0,1401	0,1283	0,1182	-0,1353	-0,4004
Mn#6	0,6794	-0,7695	0,8322	-0,8503	0,7423	-0,7031	0,8314	-0,9854	0,7981
Mn#5	0,2229	0,3940	0,0893	0,3527	-0,0895	0,5954	-0,1436	0,0615	-0,4760
P#2	-0,1254	0,1239	-0,1143	0,1600	-0,0468	-0,1678	-0,0830	0,3452	-0,2421
S#1	0,1266	0,6574	0,0989	0,5769	0,1565	0,6217	0,0240	0,1752	-0,7090
Cr#1	0,3443	0,1227	-0,0151	0,2144	-0,6299	0,2879	-0,6005	0,4273	-0,5463
Cr#13	0,6084	0,0610	0,3165	0,0980	-0,2741	0,1772	-0,2622	0,1528	-0,4946
Cr#9	0,3639	0,1255	0,0575	0,2085	-0,4830	0,1417	-0,4733	0,4382	-0,5737
Cr#2	0,1569	0,5179	-0,1387	0,5654	-0,5289	0,6050	-0,5819	0,5753	-0,8439
Mo#1	-0,3660	-0,0059	-0,6181	0,1427	-0,9128	0,1807	-0,8361	0,5845	-0,1122
Mo#2	0,1888	-0,4543	0,2285	-0,4798	0,1560	-0,1849	0,2429	-0,5523	0,5910
Mo#4	0,8167	-0,2575	0,7115	-0,2722	0,2878	-0,3509	0,3052	-0,2574	-0,1310
Mo#3	0,8655	-0,2782	0,6536	-0,2661	0,0517	-0,2142	0,0983	-0,2091	-0,1641
Ni#13	-0,1242	-0,6804	-0,0564	-0,6239	-0,0562	-0,5949	0,0766	-0,3112	0,8085
Ni#2	0,3610	0,2022	0,2310	0,2164	-0,0246	0,0218	-0,0720	0,2644	-0,5412
Ni#4	0,4895	-0,7923	0,6269	-0,8459	0,5581	-0,6600	0,6688	-0,9017	0,8832
Ni#3	0,6086	-0,1408	0,5621	-0,2112	0,3122	0,0636	0,3256	-0,4917	0,0506
Al#5	-0,2834	0,6057	-0,1482	0,4987	0,2564	0,6344	0,1322	0,0125	-0,3252
Al#6	-0,5801	0,8432	-0,4507	0,7622	0,0659	0,7822	-0,0922	0,3451	-0,5400
As#1	0,4323	-0,5306	0,5703	-0,5562	0,5612	-0,7866	0,6013	-0,4555	0,4257
B#1	0,0473	0,5508	0,1949	0,4316	0,5184	0,3451	0,3705	-0,0187	-0,4705
Co#1	0,4142	0,0515	0,1329	0,1293	-0,3973	0,0330	-0,3824	0,3676	-0,5043
Co#2	0,7497	-0,0945	0,5834	-0,0957	0,1159	-0,1489	0,1182	-0,0827	-0,3232
Cu#1	0,2971	-0,0700	-0,0380	0,0518	-0,6441	0,0102	-0,5837	0,4336	-0,3710
Cu#2	0,0574	0,0893	-0,3027	0,2115	-0,8505	0,3493	-0,7929	0,5107	-0,3935
Cu#6	-0,1726	-0,1107	0,0757	-0,2063	0,4831	-0,0300	0,4756	-0,5161	0,4986
Cu#5	-0,4863	-0,2043	-0,2349	-0,2381	0,2362	-0,1899	0,2601	-0,2949	0,6272
Nb#1	-0,0486	0,2142	-0,0906	0,1775	-0,0938	0,4865	-0,1095	-0,0733	-0,0874
Nb#2	0,0365	0,6469	-0,1206	0,6554	-0,2446	0,5249	-0,3524	0,5770	-0,8873
Pb#2	-0,1253	0,1568	-0,0842	0,1017	0,0484	0,3945	0,0315	-0,1842	0,0678
Sn#1	-0,2828	0,8395	-0,2244	0,7722	0,1033	0,6407	-0,0664	0,4354	-0,7732
Ti#1	-0,6784	0,5753	-0,4378	0,5162	0,2165	0,2963	0,0839	0,3008	-0,2504
Ti#2	-0,6347	0,5989	-0,3983	0,5339	0,2432	0,3127	0,1039	0,2950	-0,2922
V#1	0,5031	0,2408	0,2841	0,2276	-0,1297	0,4046	-0,1569	0,0659	-0,5235
W#1	-0,5237	0,5538	-0,2858	0,4467	0,3262	0,5010	0,2028	0,0037	-0,1396
W#16	-0,3906	-0,3202	-0,1162	-0,3586	0,3418	-0,3445	0,3767	-0,3955	0,7209
W#2	-0,0769	0,3645	-0,3805	0,4398	-0,7506	0,6487	-0,7476	0,5203	-0,5398
Zr#1	0,6009	0,2074	0,3978	0,1948	-0,0256	0,2425	-0,0621	0,0797	-0,5690
Ca#1	0,1031	0,2765	0,0323	0,2972	-0,0530	0,0259	-0,1150	0,3789	-0,5185
Sb#2	-0,8805	0,8926	-0,9136	0,9272	-0,5626	0,8230	-0,6856	0,8898	-0,7217
Te#2	-0,4661	0,3820	-0,7178	0,4866	-0,9062	0,6367	-0,8956	0,6794	-0,4176
Ce#3	-0,0661	0,0066	0,1514	-0,0434	0,4981	-0,3485	0,4417	-0,0968	0,0737
La#1	-0,7779	0,1190	-0,5680	0,1088	-0,0225	0,1059	-0,0396	0,0750	0,3215
Mg#2	-0,3635	0,0630	-0,0372	-0,0472	0,5711	0,0027	0,5186	-0,3941	0,3937
Mg#3	-0,3438	0,0870	-0,0163	-0,0287	0,5938	0,0206	0,5349	-0,3974	0,3644
Zn#2	-0,5087	0,2840	-0,7426	0,4266	-0,9173	0,3278	-0,9007	0,8329	-0,4137
N#1	-0,5897	0,1528	-0,3227	0,1217	0,2642	-0,1300	0,2042	0,0902	0,1606
N#2	-0,2646	-0,3896	-0,3732	-0,2598	-0,5521	-0,3328	-0,4389	0,2426	0,3311

Legend:
0 – 0.3 weak correlation – red color,
0.3 – 0.5 moderate correlation – orange color,
0.5 – 0.7 strong correlation – yellow color,
0.7 – 1 very strong correlation – green color.

Example analysis for sample RG 14/531

REFERENCES

1. J. Paradysz, Statystyka, Wydawnictwo Akademii Ekonomicznej w Poznaniu, Poznań 2004 r.,
2. W. Szczepaniak, Metody instrumentalne w analizie chemicznej, Wydawnictwo Naukowe PWN, Warszawa 2007 r,
3. M. Wieczorowski, Teoretyczne podstawy przestrzennej analizy nierówności powierzchni, Inżynieria Maszyn, 2013,
4. A. Dera, Charakterystyka wypaleń spektrometrem w stopach stali, praca dyplomowa magisterska, Wydział Politechniczny Akademii Kaliskiej, Kalisz 2021 r.

CONTACT

Adrian Dera, MSc, Eng., Department of Mechanics and Mechanical Engineering, Polytechnic Faculty, President Stanislaw Wojciechowski University of Kalisz, pl. W. Bogusławskiego 2, 62-800 Kalisz, Poland, e-mail: a.dera@uniwersytetkaliski.edu.pl

Szymon Witczak, MSc, Eng., Department of Mechanics and Mechanical Engineering, Polytechnic Faculty, President Stanislaw Wojciechowski University of Kalisz, pl. W. Bogusławskiego 2, 62-800 Kalisz, Poland, e-mail: s.witczak@uniwersytetkaliski.edu.pl

University of Kalisz

The project is co-financed from the state budget, allocated by the Minister of Science under „Doskonała Nauka II" programme.

Ministerstwo Nauki i Szkolnictwa Wyższego